

Published in final edited form as:

Biochemistry. 2010 February 23; 49(7): 1388–1395. doi:10.1021/bi9018225.

Roles for Cationic Residues at the QA binding site of QAPRTase†

Zainab Bello‡ and Charles Grubmeyer*

Fels Institute for Cancer Research and Molecular Biology and Department of Biochemistry, Temple University School of Medicine, 3307 North Broad Street, Philadelphia, Pennsylvania 19140

Abstract

Quinolinic acid phosphoribosyltransferase (QAPRTase, EC 2.4.2.19) forms nicotinate mononucleotide (NAMN) from quinolinic acid (QA) and 5-phosphoribosyl 1-pyrophosphate (PRPP). Previously determined crystal structures of QAPRTase•QA and QAPRTase•PA•PRPP complexes show positively charged residues (Arg118, Arg152, Arg175, Lys185 and His188) lining the QA binding site. To assess the roles of these residues in the *Salmonella typhimurium* QAPRTase reaction, they were individually mutated to alanine and the recombinant proteins overexpressed and purified from a recombineered *E. coli* strain that lacks the QAPRTase gene. Gel filtration indicated that the mutations did not affect the dimeric aggregation state of the enzymes. Arg175 is critical for the QAPRTase reaction, and its mutation to alanine produced an inactive enzyme. The k_{cat} values for R152A and K185A were reduced by 33-fold and 625-fold, and binding affinity of PRPP and QA to the enzymes decreased. R152A and K185A mutants displayed 116-fold and 83-fold increases in activity towards the normally inactive QA analog, nicotinic acid (NA), indicating roles for these residues in defining the substrate specificity of QAPRTase. Moreover, K185A QAPRTase displayed a 300-fold higher k_{cat}/K_m for NA over the natural substrate QA. Pre-steady state analysis of K185A with QA revealed a burst of nucleotide formation followed by a slower steady-state rate, unlike the linear kinetics of WT. Intriguingly, pre-steady state analysis of K185A with NA produced a rapid but linear rate for NAMN formation. The result implies a critical role for Lys185 in the chemistry of the QAPRTase intermediate. Arg118 is an essential residue that reaches across the dimer interface. Mutation of Arg118 to alanine resulted in 5000-fold decrease in k_{cat} value, and a decrease in the binding affinity of QA and PRPP to R152A. Equimolar mixtures of R118A with inactive or virtually inactive mutants produced approximately 50% of the enzymatic activity of WT, establishing an interfacial role for Arg118 during catalysis.

Quinolate phosphoribosyltransferase (QAPRTase, EC 2.4.2.19) is a type II phosphoribosyltransferase (PRTase) that participates in the *de novo* biosynthesis of the pyridine coenzyme, NAD (1,2). Recently, nicotinate phosphoribosyltransferase (NAPRTase) and nicotinamide phosphoribosyltransferase (NMPRTase), involved in the salvage pathways of NAD biosynthesis, have been classified as type II PRTases (3–5). The type II PRTases catalyze the transfer of a phosphoribosyl moiety from 5-phosphoribosyl-1-pyrophosphate (PRPP) to their specific substrates. The phosphoribosyl transfer reaction catalyzed by QAPRTase is linked to an irreversible decarboxylation reaction at position 2 of the quinolinic acid (QA) ring, with no cofactor requirement (2,6).

The *nadC* gene of *Salmonella typhimurium* which encodes QAPRTase is one of the three nonessential genes involved in *de novo* NAD biosynthesis (7). Unlike the other two genes (*nadA* (L-aspartate oxidase) and *nadB* (quinolate synthase)), which are known to be regulated

†Supported by NIH grant GM48623 to CG

*To whom correspondence should be addressed. Phone: (215) 707-4495. Fax (215) 707-5529, ctg@temple.edu.

‡Present address: Department of Biological Chemistry, University of Michigan Medical School, Michigan, 48109-5606.

by the *NadI* repressor, the *nadC* gene is not genetically controlled (8). However, QAPRTase is specific for QA and cannot use its analog nicotinic acid (NA). QA differs from NA by the presence of the negatively charged carboxylate group at position 2 of the molecule (Figure 1). In the salvage pathway of NAD biosynthesis, NAPRTase converts NA to NAMN. Like QAPRTase, NAPRTase shows a high degree of specificity for its substrate, as indicated in genetic and enzymological studies (9,10). Appropriate bacterial strains carrying *nadC* (to block QAPRTase activity) or *pncB* mutations (to block NAPRTase) show auxotrophies that are not relieved by NA and QA respectively (9). Additionally, NA does not detectably inhibit QAPRTase, whereas several pyridine analogs with negative charges at the 2 position have been shown to be effective inhibitors of the enzyme (11,12). Although crystal structures are available for all the type II PRTases, it remains unknown how the enzymes discriminate among their respective substrates.

The reaction catalyzed by QAPRTase follows an ordered-sequential mechanism, in which QA binds first, followed by PRPP, releasing NAMN and then PPI (13). The phosphoribosyl transfer reaction that forms the putative quinolinate mononucleotide (QAMN) intermediate is thought to precede the decarboxylation of the QAMN to form NAMN (14; a recent theoretical study (15) has reviewed this idea). QAMN has never been isolated or synthesized, and its chemical stability and properties are unknown. Thus, it is not clear if the decarboxylation is enzymatic or spontaneous. Based on inhibition studies, the putative QAMN intermediate was proposed to decarboxylate via an ylide mechanism (12,16–17). The ylide mechanism has also been proposed for the decarboxylation of orotidine 5'-monophosphate by OMP decarboxylase, which, like QAPRTase, is an α/β barrel enzyme, and has no cofactor requirement (18). Among cofactorless decarboxylases, a lysine amino group was recently proposed to act as the initial carboxyl receptor in a bacterial oxaloacetate decarboxylase (19). Studies with model compounds showed that non-enzymatic decarboxylation of pyridine 2-carboxylic acids substituted with a carboxyl group at position 3 occurred spontaneously (16,17). However, the rate of the QAPRTase reaction is 5 orders of magnitude faster than the spontaneous decarboxylation of the model compounds. QAPRTase may thus be involved in the decarboxylation step. Positively charged residues in the active site of the enzyme might directly stabilize the negative charge at the 2-position of QA after decarboxylation of the putative QAMN intermediate (2,6).

Crystal structures of substrate-bound complexes of QAPRTase from various organisms provide insights into the structure-function relationship of the enzyme (2,6,20–22). The active site of the enzyme is located at the C-terminal α/β -barrel domain of one subunit, which is bordered by the N-terminal domain of the adjacent subunit, forming a head-to-tail, domain-swapped dimer (2). In the crystal structure of *S. typhimurium* QAPRTase, the QA binding site (Figure 2) is composed of the following positively charged residues; Arg118' (sequence numbering is based on the mature *Salmonella* enzyme; the prime designates a residue from the adjacent subunit), Arg152, Arg175, Lys185 and His188. One of the oxygen atoms of the 2-carboxylate of PA (Figure 2) forms hydrogen bonds with the amino nitrogen of Lys185 (2.8 Å) and it is 3 Å away from NH1 of Arg118'. Arg118' is involved in an extensive hydrogen bonding. The *Mycobacterium tuberculosis* QAPRTase•PA•PRPP ternary analog complex shown here demonstrated that in addition to interacting with QA, NH1 of Arg118' is within hydrogen-bonding distance of the α -phosphate of PRPP (6). The second oxygen atom of the 2-carboxylate of PA is 3.3 Å away from the N ϵ of Arg118', and forms a hydrogen bond with the mainchain N of Arg152. These residues may be important for binding of QA or exclusion of NA. Additionally, the negative charge at the 2-position of the QA ring after decarboxylation of QAMN intermediate might be stabilized indirectly, by inductive electron withdrawal through interactions of Arg152 and Arg175 (2,6). Arg175 makes a bidentate hydrogen bond with the oxygen atoms of the C3 carboxylate of PA, while the N ϵ of Arg152 is seen to interact

with one of the oxygen atoms of PA. His188 (not shown) is also in the wall of the active site, but its closest approach to QA (via the C2 carboxylate) is 8.3 Å.

The origin of the striking base specificity of QAPRTase remains a major issue. It is easiest to imagine that NA simply fails to form the panoply of hydrogen bonds that QA can. In line with this, NA is a particularly poor inhibitor of QAPRTase (11). That poor binding may extend to poor catalysis; in particular a dual interaction of Arg118' with both the 2-carboxylate of QA and the pyrophosphate portion of PRPP may allow QA to orient for catalysis, whereas NA may not. Alternatives would include the proposal that NA may be able to undergo weak and nonproductive “wrong way” binding in which the C3 carboxylate occupies the site normally bound by the 2-carboxylate of QA, with the N1 of NA now occupying the site normally occupied by the C4 of QA. In thymidylate synthase, exclusion of dCMP from the dUMP site appeared to arise by steric exclusion mediated by Asn229, but study of indiscriminant D229N mutants suggests a more complex mechanism including rearrangement of active site residues. The potential mobility of Lys185, and its somewhat “kinked” sidechain conformation, makes a role for exclusion of NA a possibility. However, examination of structures does not seem to support an alternative position of the Lys185 sidechain that blocks access to the QA site by NA.

The positively charged residues that line the QA binding site are thus base binding residues, candidates for base specificity and might act directly or indirectly stabilize the QAMN intermediate. In a recent characterization of the human QAPRTase the homologous residues were identified and preliminary characterization of mutants was reported (21). In this paper, the residues were mutated individually to alanine, in order to explore their contribution to catalysis. The kinetic characterization of the mutant enzymes with respect to WT is presented, allowing conclusions about the origin of the base specificity of the enzyme.

Materials and Methods

Materials

Materials used have been previously described (24). SDS-PAGE (14–20%) gels were from Lonza Biosciences. [¹⁴C]NA was obtained from Sigma.

Over-expression and Purification of Enzymes

Construction of ZB100, the deleted *nadC* strain of BL21(DE3) has been described (24). The QuikChange site-directed mutagenesis kit (Stratagene) was used to carry out the mutations. The following primers were used to construct the mutants: R118A (forward, G CTG ACC GGC GAG **GCG** ACG GCG CTA AAC TTT GTC; reverse, GAC AAA GTT TAG CGC CGT **CGC** CTC GCC GGT CAG C), R152A (forward, C CAG TTG CTC GAC ACG **GCG** AAA ACG CTG CCG GGT C; reverse G ACC CGG CAG CGT TTT **CGC** CGT GTC GAG CAA CTG G), K153A (forward CAG TTG CTC GAC ACG CGT **GCG** ACG CTG CCG GGT CTG CGC; reverse GCG CAG ACC CGG CAG CGT **CGC** ACG CGT GTC GAG CAA CTG), R175A (forward, C GGC GGC GCC AAT CAT **GCG** CTG GGC CTC ACT GAC G; reverse, C GTC AGT GAG GCC CAG **CGC** ATG ATT GGC GCC GCC G), K185A (forward, CTC ACT GAC **GCG** TTC CTG ATT GCG GAA AAC CAT ATT ATC GCC TCC; reverse, GGA GGC GAT AAT ATG GTT TTC **CGC** AAT CAG GAA CGC GTC AGT GAG) and H188A (forward, C GCG TTC CTG ATT AAA GAA AAC **GCG** ATT ATC GCC TCC GGT TCG GTT C; reverse, G AAC CGA ACC GGA GGC GAT AAT **CGC** GTT TTC TTT AAT CAG GAA CGC G) with the mutated codon in bold. The ZB100 strain used for protein expression was transformed with the mutant plasmids following standard procedure. The mutant enzymes were over-expressed and purified as previously described (24).

Characterization of Mutant QAPRTases

The aggregation state, equilibrium binding of [¹⁴C]PRPP and [³H]QA and QAPRTase activity of WT and mutants enzyme forms was assayed as described (24).

Pre-steady State Measurements

Pre-steady state analysis for the formation of [³H]NAMN and [¹⁴C]NAMN using [³H]QA and [¹⁴C]NA as substrates, respectively, were carried out. Rapid quench experiments were carried out at 25°C in buffer QA using RQF-3 Chemical-Quench-Flow apparatus (KinTek Instruments). Reactions were initiated when 15 µL enzyme (80 µM) pre-equilibrated with 2 mM [³H]QA or [¹⁴C]NA was mixed with 15 µL PRPP (8 mM) in buffer QA. Reaction times ranged from 1 s to 10 min. Reactions were quenched with 2 M HCl and collected in 1.5 ml Eppendorf tubes. After all the samples were collected, the tubes were centrifuged at 3000 x g for 2 min to remove the denatured protein. Aliquots of 10 µL of the quenched sample were spotted and chromatographed on 3MM Whatman paper with a 4:6 mixture of 1M ammonium acetate and 95% ethanol. Under the given conditions, QA and NAMN have R_f values of 0.25 and 0.4, respectively. The [³H]QA and [³H]NAMN were quantitated as described previously (24). Control experiments in the absence of enzyme in which the reaction was quenched with HCl determined the background activity. Formation of NAMN by R118A and K185A using [³H]QA were performed by manual mixing. The data for the product formed by the reaction of K185A with [³H]QA was fitted to the burst equation 1 (25).

$$[Y]=A(1 - e^{-k_1 t})+k_{ss} \quad (1)$$

where A is the burst amplitude, k_1 the pre-steady-state rate constant for product formation, t , time, and k_{ss} the steady-state rate of product formation.

Alternative Substrates for Mutant Enzymes

2,4-pyridinedicarboxylic acid, 2,5-pyridinedicarboxylic acid, 2,6-pyridinedicarboxylic acid, 3,4-pyridinedicarboxylic acid, 3,5-pyridinedicarboxylic acid, nicotinamide, pyridine-4-carboxylic acid, 6-aminonicotinic acid and NA were incubated individually, with WT and mutant enzymes under standard radiolabel assay conditions (24). Reaction products were visualized under 254 nm UV light after chromatographic separation of products from the transfer assay. The reaction mixture contained 500 µg of mutant enzyme, 0.5 mM of alternative substrate and 2mM PRPP in a 200 µL reaction volume. The reaction mixtures were incubated for 3 h at 30°C, inactivated with 2M HCl and centrifuged for 5 min (14 800 × g) in a microcentrifuge. The supernatant (25 µL) was applied to 3MM Whatman paper and developed as described (24). The formation of [¹⁴C]NAMN by WT and R152A using [¹⁴C]NA as a substrate was measured by the radiolabel transfer assay.

Restoration of Activities of by Mutant Enzymes by R118A Complementation

Heterodimers of R118A with mutant enzymes (R152A, K153A, R175A and K185A) were formed individually by mixing equal concentrations (2 mg/mL) of the enzymes in buffer QA containing 1 mM DTT, and incubating them for 3 h in ice. The enzymatic activities of the heterodimers were determined by the standard spectrophotometric assay.

RESULTS

The Hydrogen Bond Network in the QA Binding Site

The cationic nature of the quinolate binding sites of all known QAPRTases has been noted (2,6,21–22). Close examination of X-ray structures reveals an intricate web of deduced hydrogen bonding, exemplified by the structure of the *Mycobacterium* ternary substrates analog complex in Figure 2, which is similar to a recent structure of the yeast enzyme (22; bond lengths are for the complex shown here, and vary somewhat with other complexes, analogs and species). The sidechain of Lys185 forms a 2.8 Å hydrogen bond to one C2 carboxylate oxygen, which also interacts (2.95 Å) with NH1 of Arg118'. Arg118 also interacts through its NE with the other C2 carboxylate oxygen (3.3 Å) and, via NH1, with an α -phosphate oxygen of PRPP (2.9 Å). The C2 carboxylate forms a fourth deduced hydrogen bond (3.1 Å) with Arg152 through the mainchain N of the latter. At the C3 carboxylate, three apparent hydrogen bonds, from NE of Arg152 (2.8 Å), and from NE (3.0 Å) and NH1 (3.1 Å) are formed. Thus, each of the two carboxylates and each of the Arg residues makes multidentate hydrogen bonds that could serve to read substrate identity. Lys185, which forms a single hydrogen bond, appears more free to move, and a recent structure of the binary complex of QA with the yeast enzyme shows Lys185 interacting via a water molecule with a C3 carboxylate oxygen (22).

Examination of a large sequence library (Materials and Methods) showed that the residues lining the QA site were highly conserved (Figure 3). Arg152, Lys153, Arg175 and His188 were all absolutely conserved. Arg118 and Lys185 were conserved, except for replacement by Lys and Phe, respectively in *Rhodospseudomonas palustris*. The extreme sequence conservation is in keeping with important functional roles.

Expression and Purification of Mutant QAPRTases

The over-expression and purification of the mutant enzymes produced 200–250 mg of protein per 6 L of culture, and were similar to that of the WT enzyme. The mutant enzymes appeared homogeneous as assessed by SDS-PAGE.

Aggregation State of Mutant QAPRTases

Gel filtration of the mutant enzymes under native conditions was performed on a Superdex 200 column. All mutant enzymes eluted at the same position as WT (data not shown), with similar peak-widths at half height, indicating that the enzymes were stably dimeric with molecular mass of 65 kDa, as predicted for WT (64 856 (26)).

Steady-state Kinetic Measurement for Mutants

Mutation of the residues lining the QA binding site had large impacts on catalytic activity. The steady-state kinetic constants for WT and mutant enzymes are summarized in Table 1. The mutation of Arg118 diminished $k_{\text{cat}}/K_{\text{m,PRPP}}$ for R118A by 281 000-fold compared to WT, indicating the importance of Arg118 in catalysis. This reduction was a result of a 5 000-fold lower k_{cat} value and approximately 55-fold elevated $K_{\text{m,PRPP}}$ value. The $k_{\text{cat}}/K_{\text{m,QA}}$ for R118A is reduced by 25 000-fold, due to the 5 000-fold reduction in k_{cat} and a 5-fold increase in $K_{\text{m,QA}}$ value.

Lys185 and Arg152, which interact with the 2-carboxylate and 3-carboxylate of QA, respectively, gave, as expected, decreases in activity for their mutations. Removal of the sidechain of Lys185 resulted in a 625-fold decrease in k_{cat} , with a 38-fold higher $K_{\text{m,PRPP}}$ and a 55-fold increase in $K_{\text{m,QA}}$ causing 34 000-fold decrease in $k_{\text{cat}}/K_{\text{m,QA}}$ and 25 000-fold reduction in $k_{\text{cat}}/K_{\text{m,PRPP}}$ value. For R152A, k_{cat} decreased by 33-fold, with a 15-fold increase in $K_{\text{m,PRPP}}$ and 10-fold increase in $K_{\text{m,QA}}$ leading to a 500-fold and 370-fold reduction in $k_{\text{cat}}/K_{\text{m,PRPP}}$ and $k_{\text{cat}}/K_{\text{m,QA}}$, respectively.

No measurable activity was detected for R175A, indicating that Arg175 is essential for catalysis. The undetectable activity of R175A like that of K153A (24) suggests that activities of other extremely sluggish mutants described here and in the preceding paper (24) are intrinsic to those mutant enzymes and not a result of contamination by active enzymes.

Mutation of the absolutely conserved His188 to alanine did not affect the ability of the enzyme to catalyze the QAPRTase reaction, as the k_{cat} was similar to that of WT. The $K_{\text{m,PRPP}}$ value increased by 10-fold, leading to a 10-fold reduction in $k_{\text{cat}}/K_{\text{m,PRPP}}$ H188A. With the exception of His188, the steady state results indicate that all the residues at the QA binding site of QAPRTase are important for catalysis.

Binding of PRPP and QA to the Mutant Enzymes

The effect on formation of binary complexes of mutant QAPRTase was determined by equilibrium binding experiments with [^3H]QA and [^{14}C]PRPP by centrifugal dialysis (Table 1). Surprisingly, a reduced binding affinity for PRPP was observed for all the mutant enzymes, though most of their mutated residues do not directly interact with PRPP as demonstrated from the crystal structures. A 10-fold increase was measured for $K_{\text{D,PRPP}}$ for H188A, in agreement with its K_{m} value. The $K_{\text{D,PRPP}}$ for R152A was approximately 1mM, almost 18-fold higher than WT and in agreement with its $K_{\text{m,PRPP}}$ value. The binding of [^{14}C]PRPP to R118A, R175A and K185A mutant enzymes was not detected by centrifugal dialysis, indicating $K_{\text{D,PRPP}}$ values that are greater than 1mM.

The binding of PRPP to the mutants in the presence of the QA analog, PA, which tightens binding of PRPP in WT, had no effect on the K_{D} values of PRPP (Data not shown).

The K_{D} value of QA for R152A was 260 μM , 10-fold higher than that of WT and consistent with its K_{m} value. For the binding of [^3H]QA to R118A, the K_{D} value measured is represented by Scatchard analysis shown in Fig 4. Consistent with the $K_{\text{m,QA}}$, a 5-fold higher K_{D} value for QA was measured for R118A. Binding of [^3H]QA was not detected for R175A and K185A mutant enzymes, indicating K_{D} values greater than 1 mM.

Alternative substrates

Alternative substrates were employed to test whether there was a change in base specificity of mutant QAPRTase. To assess the contribution of Arg152 and Lys185 in substrate discrimination, the ability of their respective alanine mutants to carry out the QAPRTase reaction was tested using various pyridine analogs. With the exception of NA and 6-aminonicotinic acid, all other QA analogs investigated were not detectably utilized by the mutant enzymes. Formation of NAMN by WT enzyme using NA as a substrate was detected by the radiolabel transfer assay. The specific activity of WT with NA at 1 mM and 2 mM PRPP was 0.0006 Umg^{-1} . This rate represents a 2000-fold reduction in comparison to its activity of 1.2 Umg^{-1} with 1 mM QA as the substrate. The specificity of R152A for QA and NA is more relaxed than that of WT. A specific activity of 0.07 Umg^{-1} was measured for the reaction of R152A with NA versus 0.1 Umg^{-1} using the natural QA substrate. R152A uses NA 116-fold better than WT does. Detailed steady state kinetic analysis for WT or R152A with NA was not performed.

K185A exhibited an 83-fold higher specific activity for its ability to utilize NA than the WT enzyme did with NA as a substrate. Remarkably, K185A showed a strong preference for NA over QA. Its activity with NA was sufficient to allow measurement of kinetic parameters (Table 2) by the spectrophotometric assay. A 31-fold elevation was observed in $k_{\text{cat,NA}}$ compared to the $k_{\text{cat,QA}}$ value for the mutant enzyme. The $K_{\text{m,NA}}$ value for K185A decreased by 10-fold and $K_{\text{m,PRPP(NA)}}$ decreased by 6-fold in comparison to the respective K_{m} values with the natural

QA substrate. The values of $k_{cat}/K_{m,NA}$ and $k_{cat}/K_{m,PRPP(NA)}$ are greater by 300-fold and 178-fold, respectively, in comparison to the values with QA as the substrate. K185A was the only mutant to detectably utilize 6-aminonicotinic acid as a substrate.

Pre-steady State Kinetics

It has previously been shown that the chemistry step in the QAPRTase reaction is rate limiting as evidenced from the linear rate in NAMN formation in the pre-steady state (13,24). The pre-steady state rate of NAMN formation by R118A using QA was measured by the manually quenched radiolabel transfer method. The initial rate of NAMN formation was linear, at $2 \times 10^{-5} \text{ s}^{-1}$, consistent with the steady state k_{cat} value ($2.4 \times 10^{-4} \text{ s}^{-1}$). For R152A using QA, the initial rate of NAMN formation was also linear at 0.1 s^{-1} , consistent with its steady state k_{cat} value (Figure 5).

For the K185A mutant, chemical-quench experiments performed with [^3H]QA as the substrate revealed a pre-steady state burst of [^3H]NAMN formation, followed by a slow linear rate (Figure 6). The scatter in the data is due to the low activity of the mutant enzyme. Nevertheless, the existence of a pre-steady state burst was reproducible, with an amplitude of $0.9 \pm 0.1 \text{ mol } [^3\text{H}]\text{NAMN/mol of K185A}$. A relatively fast pre-steady state rate of 0.01 s^{-1} , and a slower steady state rate of 0.00013 s^{-1} (0.008 min^{-1}) provided a good fit to the data. In contrast to WT, the presence of a burst of [^3H]NAMN formation by K185A when utilizing [^3H]QA indicates a relatively fast chemistry step for the mutant enzyme, with either product release or further processing providing the rate-limitation.

To confirm this implication, rapid quench experiments were performed with K185A, using [^{14}C]NA as the substrate. In direct contrast to the reaction of K185A with [^3H]QA, the pre-steady state result of K185A with [^{14}C]NA showed no burst of NAMN formation (Figure 7). The initial rate was linear at 0.03 s^{-1} , in agreement with the steady state k_{cat} value for NA (0.05 s^{-1}), and in particular, in rough agreement with the pre-steady burst state rate (0.01 s^{-1}) of product formation for the reaction of K185A with QA. The result of the reaction of K185A with NA suggests that the release of NAMN as observed for WT is not rate-limiting in the use of QA by this mutant. Therefore, it must be that for the reaction of K185A with QA, an intermediate was formed, whose subsequent reaction or release was rate-limiting.

The burst of on-enzyme product formation by K185A with [^3H]QA suggests the existence of an intermediate whose further reaction may limit the turnover. On paper chromatography, the behavior of the products from the reaction of K185A with [^3H]QA was similar to that of NAMN.

Restoration of enzymatic activity by mutant complementation

In the *S. typhimurium* QAPRTase dimer, Arg118' interacts with QA across the subunit interface. R118A was used as a probe in complementation experiments with other debilitated or inactive mutant enzymes, to test the importance of this interfacial participation. Incubation of equal molar concentrations of R118A with R175A resulted in restoration of enzymatic activity (Figure 8). Similar results were observed with R152A and K185A. The restoration of activity was maximal within about 2–3 hrs. The activities of individual mutants and the activities of equimolar mixtures of R118A with mutant enzymes are presented in Table 3, as percentages of the activity of WT enzyme. The general observation is that mixing R118A with all poorly active or with inactive mutants restored activity. The R118A mutant enzyme also complemented other poorly active mutants (E214A, E214D, K153A and K284) described in the preceding paper. However, mixing binary combinations from among R152A, K153A, R175A, E214A, E214D and K284A did not restore enzyme activity (Unpublished results). Because the enhanced activity was observed only in the presence of R118A, it is most likely

associated with formation of heterodimers between the two mutants. Because the activities of the equilibrated heterodimeric mutants were about 50% of WT, the most logical explanation is that one of the two active sites of the dimer can function at full activity with the other in an inactive state, and that heterodimers are preferred in mixtures of R118A with the other mutants.

DISCUSSION

The site-directed mutagenic investigation of the conserved residues at the QA binding site of QAPRTase showed that the interactions made by the residues are important for binding and catalysis. Lys185 most likely plays a direct chemical role in the stability of the QAMN ylide intermediate in the decarboxylation step, and it is a substrate specificity determinant for QAPRTase. Arg152 functions in QA binding and substrate discrimination. The very low activities of the enzyme mutated at Arg175 implied that the residue is essential and might play a role in both QA and PRPP binding. The importance of head to tail domain swapping (3) in QAPRTase is highlighted by Arg118' as one of the critical participants across the dimer interface.

The hydrogen bond provided to the 2-carboxylate of QA by Lys185 appears by design to bind QA and confer base specificity for QAPRTase. The Lys185 sidechain is one that makes a notable conformational change between different complexes. In the *Mycobacterium* apoenzyme structure, the sidechain amino group lies close to the carboxylates of Asp186 and Asn187. In the *Salmonella* QA binary complex, the sidechain has repositioned and compacted to bind to the QA 2-carboxylate. In neither state does the sidechain position appear to preclude base NA binding. The interaction at C2 could potentially stabilize the negative charge at the 2 position on the putative QAMN ylide intermediate that results from decarboxylation. The major catalytic role of Lys185 is demonstrated by the significant decrease in catalysis by K185A. Ablation of the Lys185 sidechain to eliminate its interactions with the 2-carboxylate of QA resulted in a weakened binding affinity for QA, an inability to discriminate against NA, and therefore a lack of QA specificity. The base specificity of K185A is the reverse of WT, with WT favoring QA over NA by 2000-fold and K185A exhibiting a 300-fold increase in catalytic efficiency for NA over QA. The reverse base discrimination by K185A enzyme clearly supports a major role for Arg152 in QA binding and specificity. The role of Lys185 in substrate determination reconciles with the change in conformation of Lys185, as observed in the crystal structure of the *Mycobacterium* enzyme upon binding of QA (6).

The weak binding affinities of R152A and K185A enzymes for QA suggests roles for these residues in binding QA. The role of Arg152 and Lys185 in catalytic substrate discrimination was addressed from the ability of R152A and K185A to utilize NA as a substrate.

The pre-steady state burst observed for K185A when QA is utilized as the substrate indicated that formation of an initial product was fast, and either its release or further modification was slow. However, the rapid linear reaction of K185A using NA as the substrate indicated a difference in product formation. If the initial-burst product of K185A reaction with QA were NAMN, its further kinetic behavior would be similar to the product of the K185A reaction with NA, which is without question NAMN. The presence of a slower steady state rate for the reaction of K185A with QA implied that the product that formed was not NAMN. An explanation of the burst of product formation for the reaction of K185A with QA is that the putative QAMN intermediate was formed, and either the decarboxylation of QAMN or its release into solution is the rate limiting step. Attempts to detect the QAMN intermediate were unsuccessful. The unstable nature of the putative QAMN intermediate might not have permitted its capture under the current isolation procedure. The pre-steady state experiment with K185A strongly suggests that Lys185 participates in the decarboxylation step of QAPRTase, and most likely uses its positive charge to stabilize the negative charge of QAMN

ylide intermediate. Lysine residues are known to be carbamoylated by carbon dioxide, usually to form a catalytically stable part of a metal-ion binding site. We note with interest the possibility that a lysine residue acts catalytically covalently accepts the initial carbon dioxide of *Vibrio cholerae* oxaloacetate decarboxylase (19). A water molecule found associated with the amino of Lys185 noted in some complexes of the yeast QAPRTase (22) could potentially represent a carboxy-lysine.

The importance of Arg118' in catalysis is supported by several results. First, the location of Arg118 within the active site, forming hydrogen bonds to both substrates, but stretching across the subunit in crystal structures suggested a catalytic role. Second, sequence analysis showed absolute conservation of Arg118'. Third, mutation to alanine resulted in a dramatic decrease in the catalytic efficiency for PRPP due to the reduced k_{cat} and a higher K_m value for PRPP. Finally, the undetectable binding of PRPP to R118A strongly indicates an important role for Arg118' in PRPP binding.

The observed restoration of the activity of inactive and poorly active mutants when mixed with R118A supports the structural studies in the interfacial participation of Arg118' in catalysis. Dimerization facilitates proper structural alignment of the otherwise distant and essential Arg118' residue from the adjacent subunit in the active site of QAPRTase. Earlier work by Ozturk *et al.* (27) has also shown that a type I PRTase, OPRTase, possesses this property of active site sharing of residues from the adjacent subunit. OPRTase has a flexible loop containing the Lys103 residue that is required for activity. Like QAPRTase in capping the enzyme active site, the loop in OPRTase acts as a lid for the active site formed by the adjacent subunit of the homodimer. In the OPRTase relative HGPRTase, the homologous loop is provided by the same subunit (28).

The very weak binding of R152A and K185A mutant enzymes to PRPP was unexpected, for neither of the residues interact directly with PRPP. The likeliest explanation for this observation is that the web of hydrogen bonds formed by residues interacting with QA (Figure 2) was disrupted, possibly via Arg118. Additionally, other residue-residue interactions appear important. In the *M. tuberculosis* QAPRTase•PA•PRPPC ternary complex, Arg152, which does not interact with PRPP is sequence adjacent to Lys153, which does. Arg152 is also seen to interact with the main-chain of Asn122', which in turn, forms a hydrogen bond with main chain of Arg118'. Lys185, which does not interact with PRPP, is adjacent to Asp173, which does.

Abbreviations

QA	quinolinic acid
PA	phthalic acid
PRPP	5-phosphoribosyl-1-pyrophosphate
NAMN	nicotinate mononucleotide
PPi	pyrophosphate
NAPRTase	nicotinate phosphoribosyltransferase
QAMN	quinolinate mononucleotide
PRPCP	5-phosphoribosyl-1-(β -methylene)pyrophosphate

References

1. Musick WD. Structural features of the phosphoribosyltransferases and their relationship to the human deficiency disorders of purine and pyrimidine metabolism. *CRC Crit Rev Biochem* 1981;11:1–34. [PubMed: 7030616]
2. Eads JC, Ozturk D, Wexler TB, Grubmeyer C, Sacchettini JC. A new function for a common fold: the crystal structure of quinolinic acid phosphoribosyltransferase. *Structure* 1997;5:47–58. [PubMed: 9016724]
3. Chappie JS, Canaves JM, Han GW, Rife CL, Xu Q, Stevens RC. The structure of a eukaryotic nicotinic acid phosphoribosyltransferase reveals structural heterogeneity among type II PRTases. *Structure* 2005;13:1385–1396. [PubMed: 16154095]
4. Shin DH, Oganessian N, Jancarik J, Yokota H, Kim R, Kim SH. Crystal structure of a nicotinate phosphoribosyltransferase from *Thermoplasma acidophilum*. *J Biol Chem* 2005;280:18326–18335. [PubMed: 15753098]
5. Wang T, Zhang X, Bheda P, Revollo JR, Imai S, Wolberger C. Structure of Nampt/PBEF/visfatin, a mammalian NAD⁺ biosynthetic enzyme. *Nat Struct Mol Biol* 2006;13:661–662. [PubMed: 16783373]
6. Sharma V, Grubmeyer C, Sacchettini JC. Crystal structure of quinolinic acid phosphoribosyltransferase from *Mycobacterium tuberculosis*: a potential TB drug target. *Structure* 1998;6:1587–1599. [PubMed: 9862811]
7. Foster JW, Moat AG. Mapping and characterization of the *nad* genes in *Salmonella typhimurium* LT-2. *J Bacteriol* 1978;133:775–779. [PubMed: 203571]
8. Holley EA, Foster JW. Bacteriophage P22 as a vector for Mu mutagenesis in *Salmonella typhimurium*: isolation of *nad-lac* and *pnc-lac* gene fusions. *J Bacteriol* 1982;152:959–962. [PubMed: 6752128]
9. Foster JW, Kinney DM, Moat AG. Pyridine nucleotide cycle of *Salmonella typhimurium*: isolation and characterization of *pncA*, *pncB*, and *pncC* mutants and utilization of exogenous nicotinamide adenine dinucleotide. *J Bacteriol* 1979;137:1165–1175. [PubMed: 220211]
10. Foster JW, Moat AG. Nicotinamide adenine dinucleotide biosynthesis and pyridine nucleotide cycle metabolism in microbial systems. *Microbiol Rev* 1980;44:83–105. [PubMed: 6997723]
11. Mann DF, Byerrum RU. Quinolinic acid phosphoribosyltransferase from castor bean endosperm. I. Purification and characterization. *J Biol Chem* 1974;249:6817–6823. [PubMed: 4422841]
12. Kalikin L, Calvo KC. Inhibition of quinolinate phosphoribosyl transferase by pyridine analogs of quinolinic acid. *Biochem Biophys Res Commun* 1988;152:559–564. [PubMed: 2452632]
13. Cao H, Pietrak BL, Grubmeyer C. Quinolinate phosphoribosyltransferase: kinetic mechanism for a type II PRTase. *Biochemistry* 2002;41:3520–3528. [PubMed: 11876660]
14. Bhatia R, Calvo KC. The sequencing expression, purification, and steady-state kinetic analysis of quinolinate phosphoribosyl transferase from *Escherichia coli*. *Arch Biochem Biophys* 1996;325:270–278. [PubMed: 8561507]
15. Rozenberg A, Lee JK. Theoretical studies of the quinolinic acid to nicotinic acid mononucleotide transformation. *J Org Chem* 2008;73:9314–9319.
16. Brown EV, Moser RJ. Further evidence as to the nature of the transition state leading to decarboxylation of 2-pyridinecarboxylic acids. Electrical effects in the transition state. *J Org Chem* 1971;36:454–457.
17. Dunn GE, Thimm HF. Kinetics and mechanism of decarboxylation of some pyridine carboxylic acids in aqueous solution. *Can J Chem* 1977;55:1342–1347.
18. Harris P, Navarro Poulsen JC, Jensen KF, Larsen S. Structural basis for the catalytic mechanism of a proficient enzyme: orotidine 5'-monophosphate decarboxylase. *Biochemistry* 2000;39:4217–4224. [PubMed: 10757968]
19. Studer R, Dahinden P, Wang WW, Auchli Y, Li X-D, Dimroth P. Crystal structure of the carboxyltransferase domain of the oxaloacetate decarboxylase Na⁺ pump from *Vibrio cholerae*. *J Mol Biol* 2007;367:547–557. [PubMed: 17270211]
20. Kim MK, Im YJ, Lee JH, Eom SH. Crystal structure of quinolinic acid phosphoribosyltransferase from *Helicobacter pylori*. *Proteins* 2006;63:252–255. [PubMed: 16419067]

21. Liu H, Woznica K, Catton G, Crawford A, Botting N, Naismith JH. Structural and kinetic characterization of quinolinate phosphoribosyltransferase (hQPRtase) from *Homo sapiens*. *J Mol Biol* 2007;373:755–763. [PubMed: 17868694]
22. di Luccio E, Wilson DK. Comprehensive X-ray structural studies of the quinolinate phosphoribosyl transferase (BNA6) from *Saccharomyces cerevisiae*. *Biochemistry* 2008;47:4039–4050. [PubMed: 18321072]
23. Guex N, Peitsch MC. SWISS-MODEL and the Swiss-Pdb Viewer: An environment for comparative protein modeling. *Electrophoresis* 1997;18:2714–2723. [PubMed: 9504803]
24. Bello ZI, Stitt BL, Grubmeyer C. Interactions at the 2 and 5 positions of 5-phosphoribosyl pyrophosphate are essential in *Salmonella typhimurium* quinolinate phosphoribosyltransferase. *Biochemistry*. 2009
25. Johnson, KA. *The Enzymes*. Academic Press, Inc; New York: 1992. Transient-state kinetic analysis of enzyme reaction pathways; p. 1-61.
26. Hughes KT, Dessen A, Gray JP, Grubmeyer C. The *Salmonella typhimurium* nadC gene: sequence determination by use of Mud-P22 and purification of quinolinate phosphoribosyltransferase. *J. Bacteriol* 1993;175:479–486.
27. Ozturk DH, Dorfman RH, Scapin G, Sacchettini JC, Grubmeyer C. Locations and functional roles of conserved lysine residues in *Salmonella typhimurium* orotate phosphoribosyltransferase. *Biochemistry* 1995;34:10755–10763. [PubMed: 7545005]
28. Eads JC, Scapin G, Xu Y, Grubmeyer C, Sacchettini JC. The crystal structure of human hypoxanthine-guanine phosphoribosyltransferase with bound GMP. *Cell* 1994;78:325–334. [PubMed: 8044844]

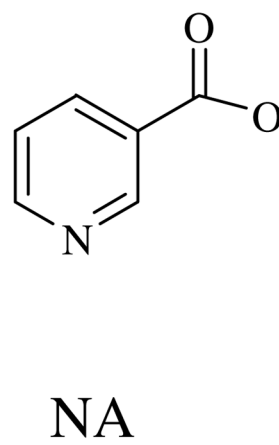
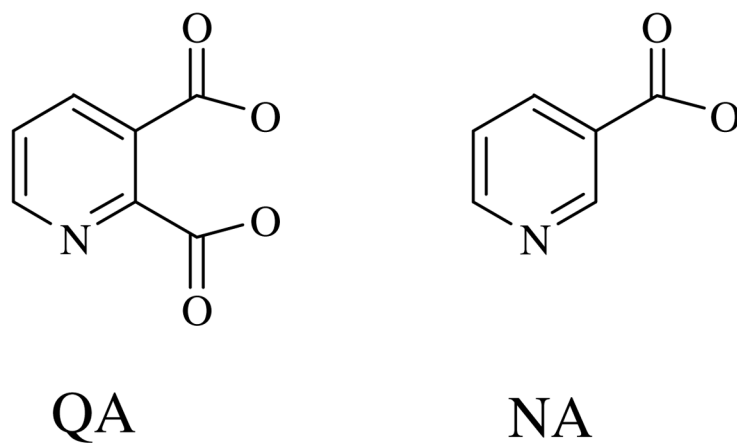


Figure 1.
Chemical structures of quinolinate and nicotinate.

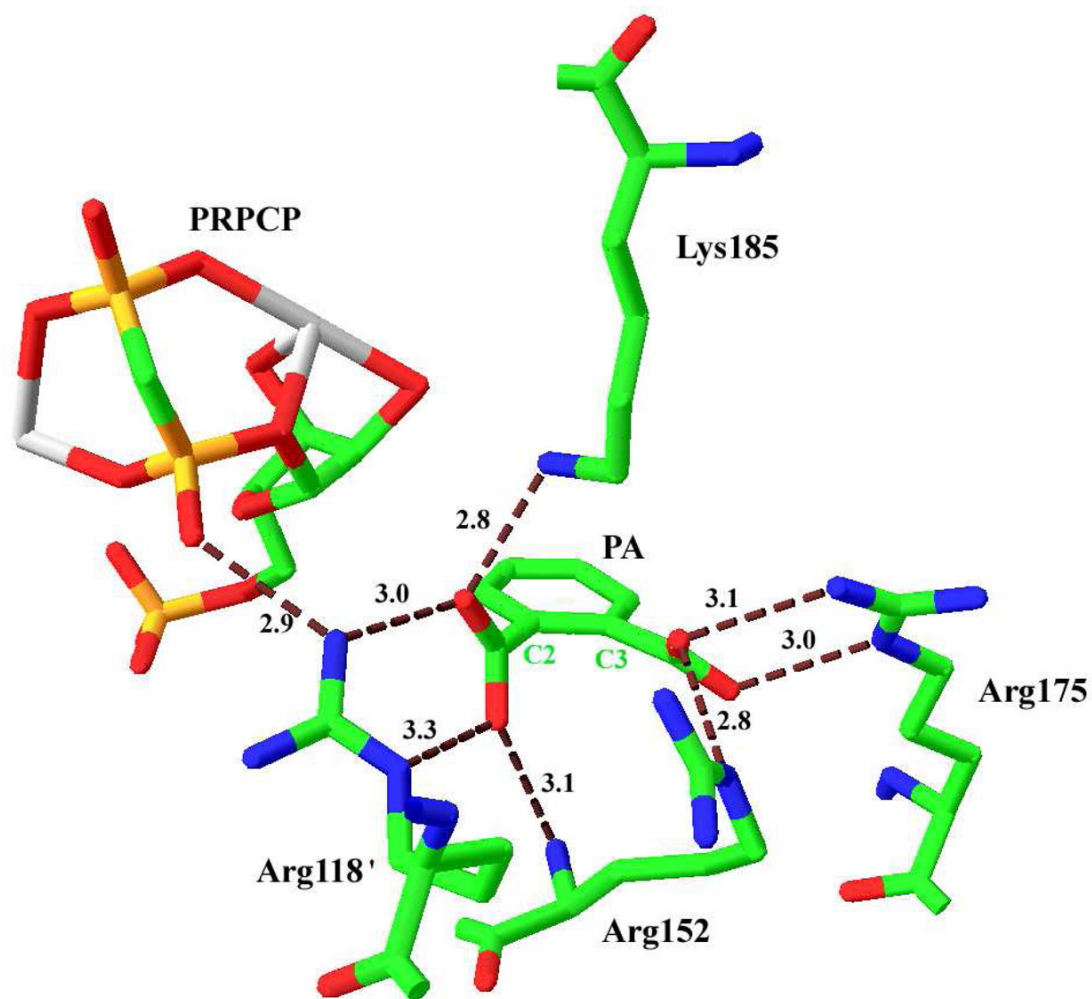
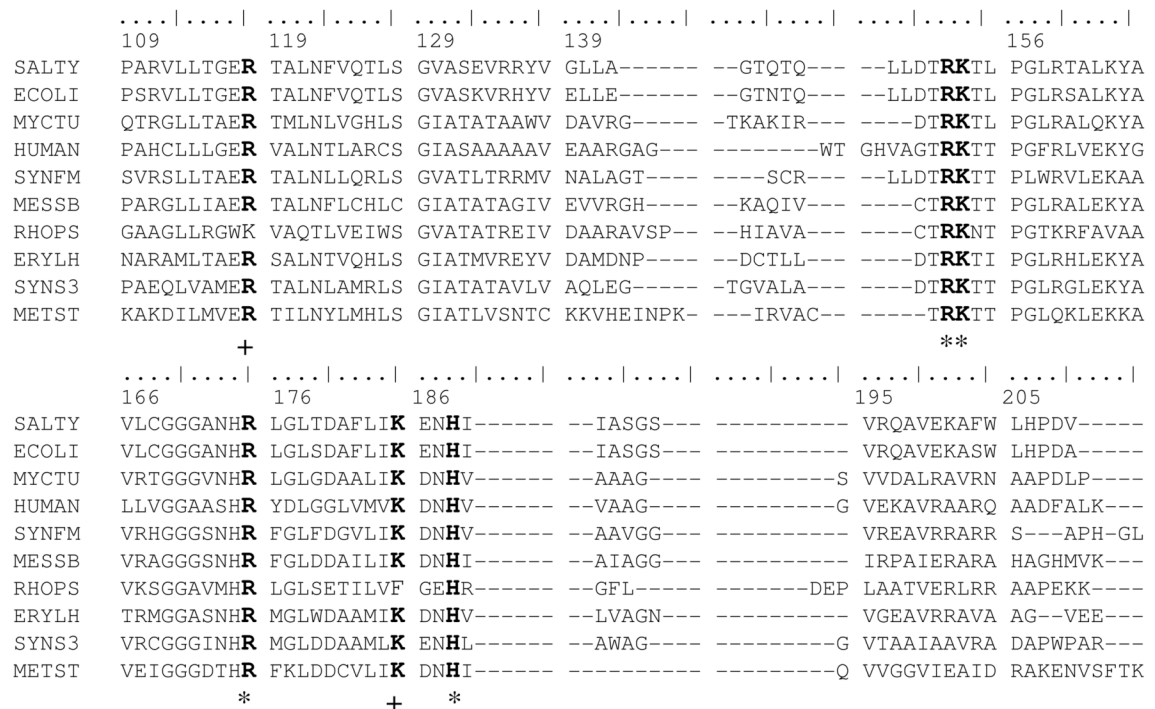


Figure 2. Binding site for QA in the *M. tuberculosis* QAPRTase•PA•PRPCP•Mn²⁺ Michaelis complex (PDB entry 1QPR). Residues that interact with QA are shown and their hydrogen-bonding distances are represented in Å. The primes on Arg118' designates residue from the adjacent subunit. C2 and C3 are designations of the homologous positions on QA. The Two Mn²⁺ are coordinated by PRPC are shown in gray. This figure was generated using SwissPDB Viewer (23).

**Figure 3.**

Partial sequence alignment of QAPRTase from various organisms. 10 of the 230 sequences aligned as described in Methods are displayed. Sequences are: SALTY, *Salmonella typhimurium* LT2; ECOLI, *Escherichia coli* K-12; MYCTU, *Mycobacterium tuberculosis* H37Rv; HUMAN, *Homo sapiens*; SYNFM, *Syntrophobacter fumaroxidans*; MESSB, *Mesorhizobium* sp. BNC1; RHOPS, *Rhodopseudomonas palustris* BisB5; ERYLH, *Erythrobacter litoralis*; SYNS3, *Synechococcus* sp. CC9311; METST, *Methanospaera stadmanae*. Residue numbering at top is from the mature *S. typhimurium* protein sequence. Conserved residues are indicated in bold, absolutely conserved residues are marked with *, and highly conserved residues are marked with + underneath the alignments.

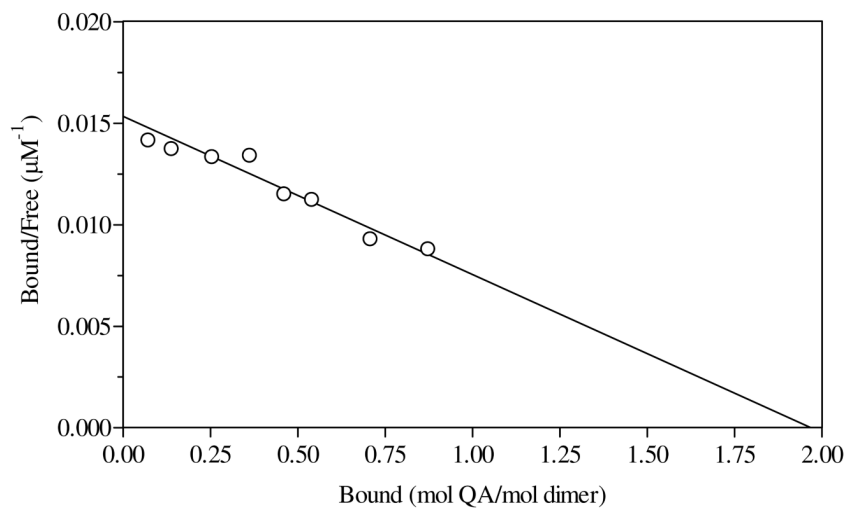


Figure 4. Scatchard plot for binding of R118A to [^3H]QA. The value of K_D was 128 μM , with an n value of 1.9 mol of [^3H]QA/mol QAPRTase dimer.

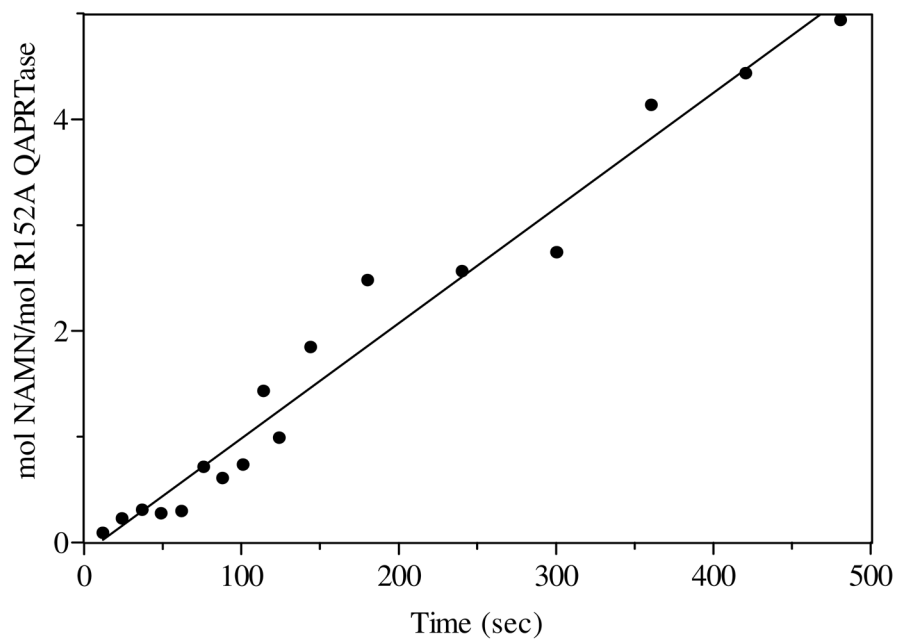


Figure 5. Pre-steady state kinetics of [^3H]NAMN formation by R152A with [^3H]QA. Rapid mixing was performed in a Kintek Chemical-Quench-Flow apparatus as described in Materials and Methods. The solid line represents a linear least square fit to the data points. The k_{cat} of the reaction was 0.1 s^{-1} .

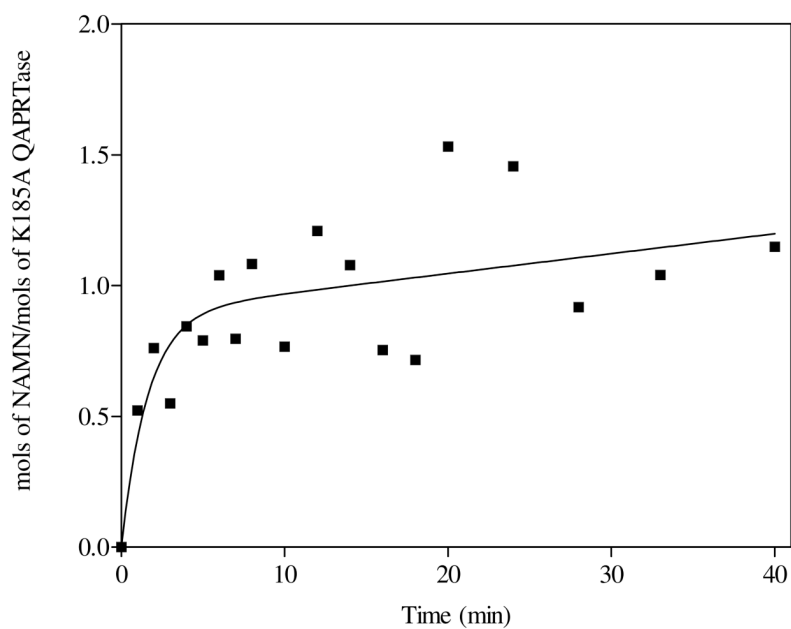


Figure 6. $[^3\text{H}]$ NAMN formation by K185A with $[^3\text{H}]$ QA in the pre-steady state. Rapid mixing was performed manually as described in Materials and Methods. The curve represents the best fit of the data to equation 1, with rate constants equal to 0.01s^{-1} and 0.00013s^{-1} , for the pre-steady and steady states, respectively.

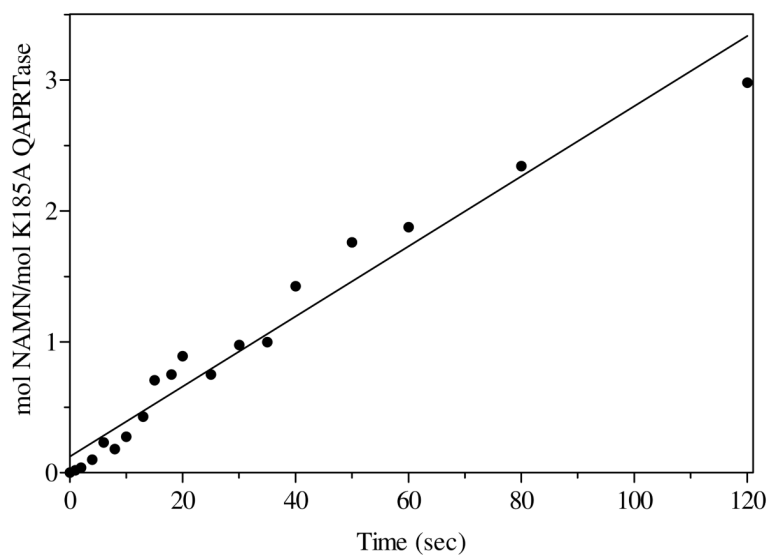


Figure 7. Pre-steady state kinetics of [^{14}C]NAMN formation by K185A with [^{14}C]NA. Rapid mixing was performed in the Kintek Chemical-Quench-Flow apparatus as described in Materials and Methods. The solid line represents a linear least square fit to the data points. The k_{cat} of the reaction was 0.03 s^{-1} .

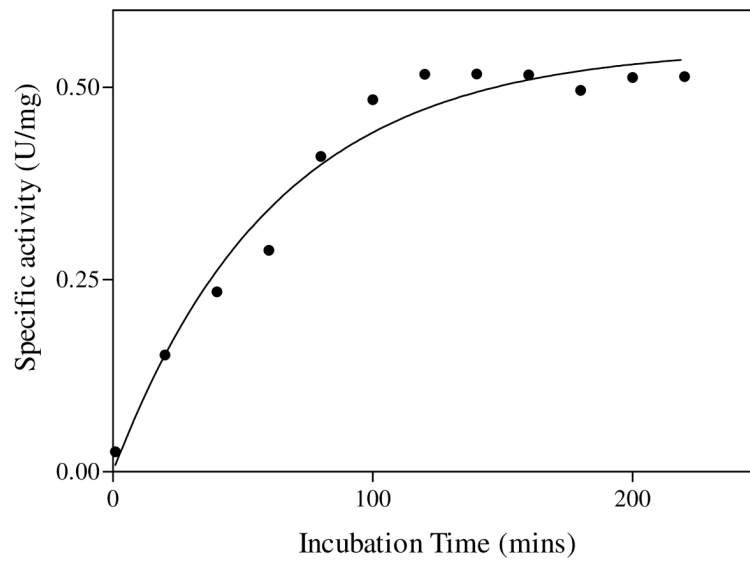


Figure 8. Time dependent complementation of inactive R175A mutant. Poorly active R118A mutant was mixed with equimolar R175A as described in Materials and Methods. The line represents a fit of data to a single exponential function.

Table 1

Steady state kinetic parameters for WT and mutant QAPRTases

kinetic constant	WT	R118A	K185A	R152A	H188A
k_{cat} (s^{-1})	1.0 ± 0.10	2.4×10^{-4}	1.6×10^{-3}	0.03	1.0 ± 0.02
K_M, QA (μM)	27 ± 6	136 ± 20	1478 ± 441	278 ± 23	67 ± 5
$k_{cat}/K_M, QA$ ($\mu M^{-1} s^{-1}$)	3.7×10^{-2}	1.5×10^{-6}	1.1×10^{-6}	1.0×10^{-4}	1.6×10^{-2}
$K_M, PRPP$ (μM)	57 ± 7	3138 ± 800	2181 ± 500	832 ± 180	547 ± 23
$k_{cat}/K_M, PRPP$ ($\mu M^{-1} s^{-1}$)	1.8×10^{-2}	6.4×10^{-8}	7.3×10^{-7}	3.5×10^{-5}	1.8×10^{-3}
K_D, QA (μM)	25 ± 7	128 ± 14	ND	261 ± 38	90 ± 15
N	2.0 ± 0.1	1.9 ± 0.1			1.8 ± 0.3
$K_D, PRPP$ (μM)	53 ± 11	ND	ND	$\sim 1000 +$	480 ± 75
					$n = 1.7 \pm 0.3$

ND, not detected

Table 2

Comparison of kinetic parameters of K185A using NA as an alternate substrate

Substrate	k_{cat} (s^{-1})	K_m (μM)	k_{cat}/K_m ($\mu M^{-1} s^{-1}$)
QA	1.6×10^{-3}	1478 ± 441	1.1×10^{-6}
NA	4.8×10^{-2}	151 ± 13	3.2×10^{-4}

Table 3

Activity of complementation mixtures containing R118A

Complementing Enzyme	Specific Activity (U mg ⁻¹)	Mixture (1:1) Tested	Specific Activity (U mg ⁻¹)
WT	1	R118A/WT	1.1
R152A	0.03	R118A/R152A	0.5
K153A	ND	R118A/K153A	0.4
R175A	ND	R118A/R175A	0.5
K185A	1.6×10^{-3}	R118A/K185A	0.5

ND, not detected

Activity of R118A was 2.4×10^{-4} U mg⁻¹